Gas-Solid Flow in Vertical Tubes

Jorge A. Pita and Sankaran Sundaresan
Mobil Research and Development Corporation, Paulsboro, NJ 08066

A computational study of fully-developed flow of gas-particle suspensions in vertical pipes was carried out, using the model proposed recently by Sinclair and Jackson (1989), to understand the predicted scale-up characteristics. It was shown that the model can capture the existence of steady-state multiplicity wherein different pressure gradients can be obtained for the same gas and solids fluxes. A pronounced and nonmonotonic variation of the pressure gradient required to achieve desired fluxes of solid and gas with tube diameter was predicted by the model, and this is explained on a physical basis. The computed results were compared with the experimental data. The model manifests an unsatisfactory degree of sensitivity to the inelasticity of the particle-particle collisions and the damping of particle-phase fluctuating motion by the gas.

Introduction

Circulating fluid beds have been applied in various industrial practices including fluid catalytic cracking (Yerushalmi and Avidan, 1985), calcination of alumina trihydrate to high-purity alumina, combustion of low-grade coal in power generation plants (Wirth, 1988), and oxidation of *n*-butane to maleic anhydride (Contractor and Sleight, 1988). A quantitative understanding of the performance of these processes hinges on our ability to capture the complex hydrodynamics observed in them. It is well known that marked segregation of particles over the cross-section occurs even in vertical flow (Bartholomew and Casagrande, 1957; Saxton and Worley, 1970; Yerushalmi et al., 1978; Youchou and Kwauk, 1980; Weinstein et al., 1984; Bader et al., 1988). Consequently, one-dimensional theoretical models (Hinze, 1952; Gidaspow and Solbrig, 1976; Leung and Jones, 1978; Ginestra et al., 1980; Arastoopour et al., 1982; Arastoopour and Cutchen, 1985; Chen et al., 1984) have required a good deal of empiricism in the form of fitted parameters which depend on the nature of the particles and the size of the tube.

Possible causes for the occurrence of lateral segregation of solids over the cross-section and the resulting large-scale mechanical effect have been explained effectively by Sinclair and Jackson (1989). In most cases of interest in circulating fluid beds, the Reynolds number for the gas flow, based on the pipe diameter, is large and the flow will be turbulent at least at low particle concentrations. Berker and Tulig (1986) adopted the view that the interaction between the particles and the turbulent eddies can lead to an uneven distribution of particles over the cross-section. However, as the effect of particles on the structure of the turbulence is not known, a heavy reliance on empiricism was inevitable.

It was pointed out by Sinclair and Jackson (1989) that in the motion of a gaseous suspension both the fluid and particle velocities have local average and random components and that the interaction of the fluctuating part of the particle motion with the mean particle motion generates stresses in the particle assembly. They constructed a mathematical model for fully-developed flow in vertical pipes taking into account only this particle-phase interaction (and neglecting the effect of turbulence) and demonstrated that such a model can reproduce qualitatively the complex variety of flow patterns known to occur in such flows. Recently, Louge et al. (1990) have expanded this model to account for the effect of turbulence; however, it appears that the particle-phase interaction is the key element required to produce lateral segregation of solids.

The present study builds on the analysis of Sinclair and Jackson (1989). These authors carried out all their simulations for a single pipe diameter (3 cm) and a single particle size (150 μm). It is of practical importance to extend their calculations to larger pipes and different particle diameters, and to compare the predictions with some experimental data. These are the objectives of the present work. It will be seen that the model of Sinclair and Jackson (1989) can capture certain multiplicity features in circulating fluid beds, which are known to be possible experimentally, but not reported, to the best of our knowledge, in any previous theoretical analysis. We will focus almost exclusively on cocurrent upflow and bring forth the complex

Permanent address of S. Sundaresan: Department of Chemical Engineering, Princeton University, Princeton, NJ 08544.

manner in which the flow behavior scales up as one increases the diameter of the pipe. Finally, we will comment on the limitations of the model.

Model Equations

The equations of motion in cylindrical coordinates for fully-developed flow take the following form (Sinclair and Jackson, 1989):

$$0 = -\epsilon_g \frac{dp}{dz} + \epsilon_g \mu_{eg}\left(\frac{d^2U_g}{dr^2} + \frac{1}{r}\frac{dU_g}{dr}\right) - \epsilon_g \rho_g g + \beta_{sg}(U_s - U_g) \quad (1)$$

$$0 = -\epsilon_s \frac{dp}{dz} + \epsilon_s \mu_{eg}\left(\frac{d^2U_g}{dr^2} + \frac{1}{r}\frac{dU_g}{dr}\right) - \epsilon_s \rho_s g + \beta_{sg}(U_g - U_s)$$

$$-\frac{1}{r}\frac{d}{dr}(r\sigma_{rz}) \quad (2)$$

$$0 = \frac{1}{r}\frac{d}{dr}(r\sigma_{rr}) - \frac{\sigma_{\theta\theta}}{r} \quad (3)$$

$$0 = \frac{1}{r}\frac{d}{dr}(r q_{PT}) + \sigma_{rz}\left(\frac{dU_s}{dr}\right) + \gamma \quad (4)$$

Equations 1 and 2 represent the axial momentum balance of gas and solid, respectively. Equation 3 is the radial momentum balance for the solid, while Eq. 4 represents the balance for the pseudothermal energy of fluctuating particle velocities. The positive direction in the z-axis is assumed to point up vertically.

A detailed account of the terms appearing in the above model equations is presented by Sinclair and Jackson (1989) and will not be repeated here. To close these equations, constitutive relations are needed for the particle-phase stress, the pseudothermal energy flux, the dissipation rate, the gas-phase effective viscosity, and the interphase drag coefficient. For the first three, we use slightly modified forms of the expressions derived by Lun and Savage (1984). For the fourth and fifth, we adopt the expressions suggested by Sinclair and Jackson (1989) and Ding and Gidaspow (1990), respectively.

$$\sigma = \rho_s \epsilon_s \theta(1 + 4\epsilon_s g_0) - \mu_b[\nabla \cdot \underline{U}_s]\underline{\underline{I}} - 2f_1\underline{\underline{S}} \quad (5)$$

$$2\underline{\underline{S}} = (\underline{\nabla}\,\underline{U}_s + \underline{\nabla}\,\underline{U}_s^T) - \frac{2}{3}(\nabla \cdot \underline{U}_s)\underline{\underline{I}} \quad (6)$$

$$q_{PT} = -f_2 \nabla\theta \quad (7)$$

$$\gamma = \frac{48}{\sqrt{\pi}}\eta(1-\eta)\frac{\rho_s \epsilon_s^2}{d_s} g_o \theta^{3/2} \quad (8)$$

$$\mu_{eg} = \mu_g(1 + 2.5\epsilon_s + 7.6\epsilon_s^2)(1 - \epsilon_s/\epsilon_o) \quad (9)$$

$$f_1 = \frac{\mu}{g_o}\left(1 + \frac{8}{5}\epsilon_s g_o\right)^2 + \frac{3}{5}\mu_b \quad (10)$$

$$f_2 = \frac{\lambda}{g_o}\left[\left(1 + \frac{12}{5}\epsilon_s g_o\right)^2 + \frac{512}{25\pi}\left(\epsilon_s g_o\right)^2\right] \quad (11)$$

$$\beta_{sg} = \frac{3}{4}C_d \cdot \frac{\epsilon_g \epsilon_s \rho_g |\underline{U}_g - \underline{U}_s|}{d_s} \cdot \epsilon_g^{-2.65} \quad (12)$$

where

$$\mu = 5m(\theta/\pi)^{1/2}/16d_s^2;\ \mu_b = 256\mu\epsilon_s^2 g_o/5\pi$$

$$\eta = (1+e)/2;\ \lambda = 75m(\theta/\pi)^{1/2}/64d_s^2;$$

$$g_o = (1 - (\epsilon_s/\epsilon_o)^{1/3})^{-1}$$

and

$$C_d = \begin{cases} \dfrac{24}{Re_g}(1 + 0.15Re_g^{0.687}) & \text{if } Re_g < 10^3 \\ 0.44 & \text{if } Re_g > 10^3 \end{cases}$$

with Re_g defined as:

$$Re_g = \epsilon_g \rho_g |\underline{U}_g - \underline{U}_s| d_s/\mu_g$$

Boundary Conditions

At the center of the tube, symmetry is assumed for all the dependent variables. The following three conditions at the tube wall, $r = R_t$, are exactly the same as those employed by Sinclair and Jackson (1989).

$$\sigma_{rz} = \frac{\phi'\sqrt{3}\,\pi\rho_s\epsilon_s\theta^{1/2}U_s}{6\epsilon_o(1 - (\epsilon_s\epsilon_o)^{1/3})} \equiv \sigma_{rz}^W \quad (13)$$

represents the stress balance at the wall for the solid phase. Here, ϕ' is a specularity factor, whose value ranges from zero, when collisions between particles and the wall are specular, to unity when incident particles are scattered diffusely.

$$q_{PT} = q_{PT}^W \equiv \frac{\sqrt{3}\,\pi\epsilon_s\rho_s\theta^{3/2}(1 - e_w^2)}{4\epsilon_o(1 - (\epsilon_s/\epsilon_o)^{1/3})} - U_s\sigma_{rz}^w \quad (14)$$

represents the exchange of pseudothermal energy between the particles and the wall. Here, e_w is the coefficient of restitution for particle-wall collisions.

For the gas phase, Sinclair and Jackson (1989) recommended the following boundary condition at $r = R_t$.

$$\left(\beta_{sg}(U_s - U_g) - \epsilon_g\rho_g g - \epsilon_g\frac{dp}{dz}\right)\delta + \mu_{eg}\epsilon_g\left.\frac{dU_g}{dr}\right|_{r=R_t} + \frac{2\mu_{eg}\theta\,U_g}{\delta\,U_t^2} = 0 \quad (15)$$

Here, $\delta = \delta_o\epsilon_s/\epsilon_o$ and $\delta_o \sim 5$; and U_t is the terminal velocity of the particle. It is instructive to examine these wall boundary conditions more closely to get a better appreciation of what they imply. For the parameter values listed in Table 1, Eq. (13) reduces to

$$U_s \approx 0.$$

Table 1. Boundary Conditions of the Tube Wall

$e = 1$	$\rho_s = 1{,}500$ kg/m^3
$d_s = 70$ μm	$\rho_g = 1.22$ kg/m^3
$\mu_g = 4 \times 10^{-5}$ kg/m·s	$e_w = 0.9$
$\phi' = 0.5$	$\epsilon_o = 0.65$

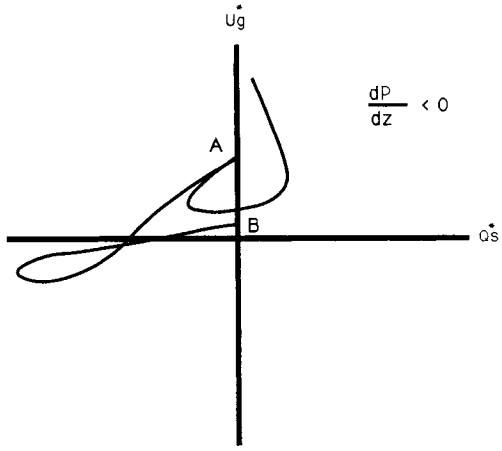

Constant dP/dz locus.

A = Classical fluidized bed

B = Packed bed

Figure 1. Gas superficial velocity vs. solid mass flux locus at constant pressure gradient.

Thus, for all practical purposes, this boundary condition is equivalent to setting the axial velocity of the particle at the wall to zero. It also implies that the specularity coefficient will have a nonnegligible effect on the model predictions, only if its value is of the order of 10^{-3} or smaller. We believe that such small values are unlikely. Next, if we examine Eq. 14, it can be concluded readily that the granular temperature at the wall will be very close to zero, independent of the value of e_w, provided that the deviation of e_w from unity is larger than 10^{-3}. Finally, it is straightforward to carry out an order of magnitude analysis of the various terms in Eqs. 1 and 2 and arrive at the conclusion that for all the conditions discussed here the effective viscosity of the gas phase plays an insignificant role. Indeed, it begins to become important only in extremely dilute and extremely high (gas) velocity pneumatic transport. The coefficient of restitution for the collision between particles is the most significant parameter in the model (besides, the easily specifiable parameters such as flow rates, particle size and density, tube size, and so on). As in the research by Sinclair and Jackson (1989), we will examine the case of perfectly elastic collisions between particles ($e = 1$) and then briefly consider the consequences of inelastic collisions between particles.

Results

Most of the results presented in this section will pertain to the flow of particles whose properties are chosen to be approximately those of the cracking catalyst. When the value of dp/dz is less than zero, the variation of the riser gas velocity (expressed as superficial velocity), U_g^*, with the cross-sectional average mass flux of the particles, Q_s^*, found by Sinclair and Jackson (1989) is shown in Figure 1. Positive values imply upflow. The radial variation of the solids fraction and the velocities corresponding to the different branches in this figure was discussed in detail by Sinclair and Jackson (1989) and will not be repeated here. They observed this trend for the flow through a 3-cm-dia. tube. We simply note that the same trends are obtained even with much larger tube diameters.

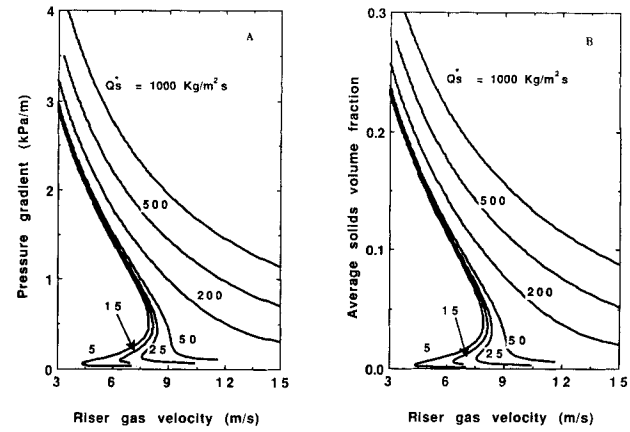

Figure 2. The variation of (a) pressure gradient ($-dp/dz$) and (b) average solid volume fraction as functions of gas velocity at different values of solid flux. Tube diameter = 1 m.

Typical Trends in Pressure Gradient and Average Solid Holdup

Although it is perhaps more elegant to present the results in a dimensionless form, we will present the results in a dimensional form commonly encountered in the literature on circulating fluid beds. Figures 2a and 2b present the axial pressure gradient ($-dp/dz$) and the (cross-sectional) average solids holdup at various values of U_g^* and Q_s^*, for a 1-m-dia. riser tube. The parameter values used in the simulations are presented in Table 1. Fluid cracking catalyst (FCC) risers operate typically with Q_s^* in the range of 300–600 kg/m^2·s and U_g^* around 15–20 m/s. In this range of Q_s^* values, the magnitude of the pressure gradient decreases monotonically with increasing riser gas velocity; and this is accompanied by a decrease in the average solids holdup. At extremely high values of U_g^* (not shown in Figure 2a), it is obtained that the magnitude of the pressure gradient will reach a minimum and then start to increase with increasing riser gas velocity (Sinclair and Jackson, 1989). This pneumatic transport regime is encountered rarely in circulating fluid bed reactors.

Figures 2a and 2b reveal that for small values of Q_s^*, there exist three possible values of ($-dp/dz$) and average solids holdup for every value of riser gas velocity, for a range of riser gas velocities. (The lowest branches of the solutions, where the pressure gradient hardly changes with riser gas velocity, are not shown completely.) To the best of our knowledge, this feature has not been reported in any previous modeling effort. The occurrence of such a multiplicity, however, is well known experimentally (Yerushalmi and Avidan, 1985; Wirth, 1988). Such values of Q_s^* are certainly of practical relevance in contexts such as circulating fluid bed combustors and maleic anhydride synthesis reactors.

Radial Variation of Solid Volume Fraction, etc.

At all U_g^* and Q_s^* value shown in Figures 2a and 2b, profound radial variations in the solids fraction, the velocities, and the

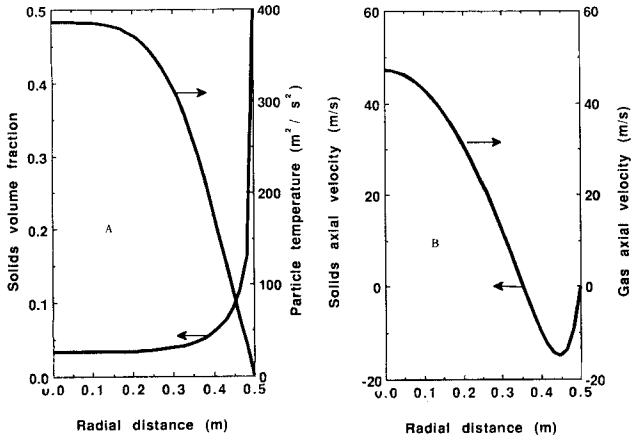

Figure 3. The radial variation of (a) the particle volume fraction and the granular temperature, and (b) the axial velocities of the two phases; upper steady state.

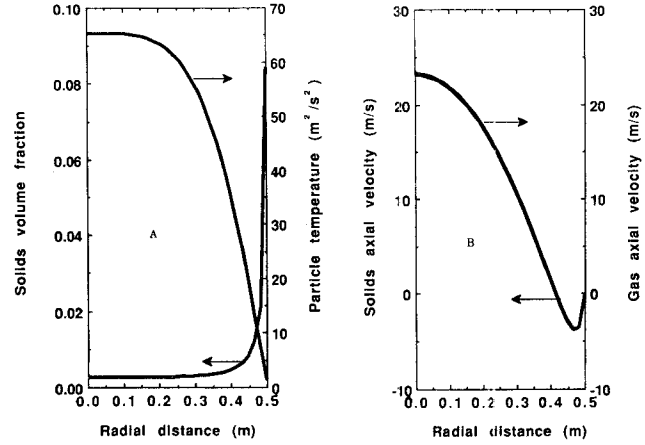

Figure 5. The radial variation of (a) the particle volume fraction and the granular temperature, and (b) the axial velocities of the two phases; lower steady state.

granular temperature (also referred to as the particle temperature) are obtained. Figures 3, 4 and 5 show the radial variation of these quantities corresponding to the three solutions for $Q_s^*=25$ kg/m^2·s and $U_g^*=8$ m/s. It can be seen that all the three branches show similar radial variations, with a downflow of solid and gas in the vicinity of the wall and an upflow in the core region. The granular temperature is very high in the core and it decreases sharply to a small value near the wall. This is accompanied by an inverse variation of the solid volume fraction. Noting that $3\theta=\langle U_s'^2\rangle$, where U_s' is the (characteristic) magnitude of the fluctuating component of the solid velocity, it can be extracted from Figures 3 to 5 that the fluctuating component of the solid velocity in the center of the tube is of the same order to magnitude as the mean axial velocity of solid there.

Extent of Recirculation

To get a better appreciation of the extent of recirculation in the riser tube, the results of Figures 2a and 2b are replotted in Figures 6a and 6b, where the net upflow (of the gas and solid, respectively) in the riser divided by the upflow in the core region is plotted against the riser gas velocity. Here, the "core" is defined as the region where the axial velocity points up. The size of the core region will, therefore, differ for different operating points. A value of unity for the quantity plotted as ordinate in Figures 6a and 6b corresponds to no recirculation. A very large recirculation of the solid is clearly evident (Figure 6b). The recirculation in the gas phase (Figure 6a) is large as well, but smaller than that for the solid phase.

Effect of Catalyst/Oil Ratio

In the context of FCC risers, the operating regions are usually characterized in terms of the so-called catalyst/oil (mass ratio). The gas phase is formed upon vaporization of the oils, so that for our analysis we can view this ratio as $[Q_s^*/\rho_g U_g^*]$. Values in the range of 6 to 15 are common for this ratio. Figures 7a and 7b show the variation of $(-dp/dz)$ and average solid holdup as a function of the riser gas velocity for various values of catalyst/oil ratios. On the lefthand limb of Figure 7a, the

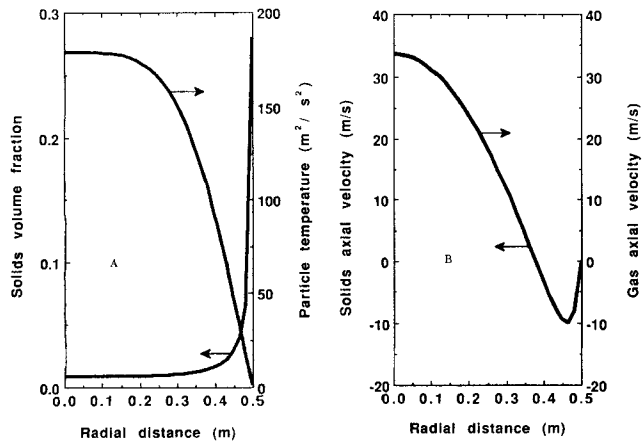

Figure 4. The radial variation of (a) the particle volume fraction and the granular temperature, and (b) the axial velocities of the two phases; middle steady state.

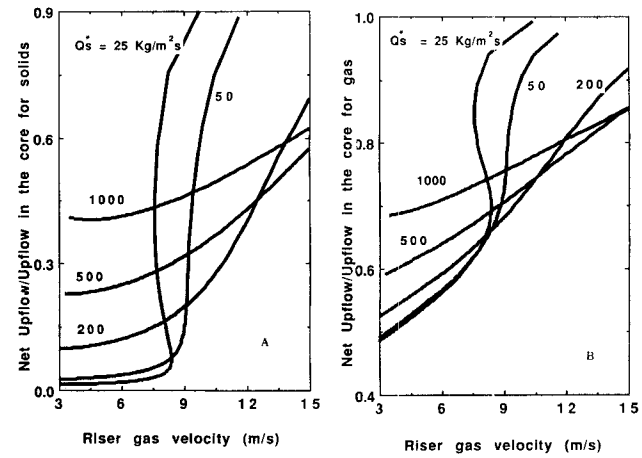

Figure 6. Extent of recirculation in the riser tube. (a) gas phase; (b) solid phase. Tube diameter = 1 m.

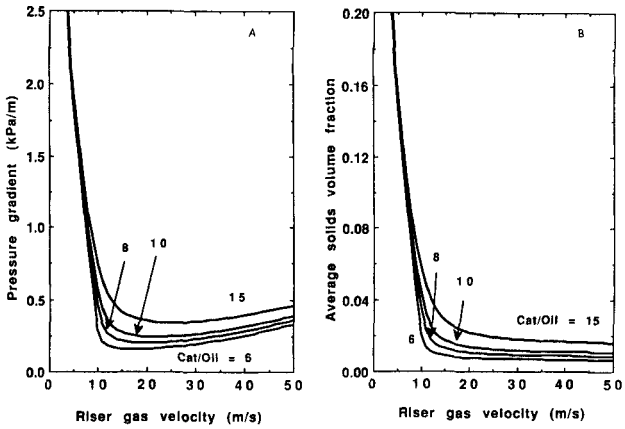

Figure 7. The variation of (a) pressure gradient ($-dp/dz$) and (b) average solid volume fraction as functions of gas velocity at different values of the solid mass flux divided by the gas mass flux (referred to as cat/oil ratio). Tube diameter = 1 m.

pressure gradient is due predominantly to the weight of the solids. This is not so in the righthand limb, where a sharp increase in the pressure gradient is predicted while the solid holdup is roughly constant. (Although the results presented in these figures are only for riser gas velocities below 50 m/s, computations were carried out for riser gas velocities up to 150 m/s. It was found that the pressure gradient continued to rise with the riser gas velocity, while the solids holdup did not.) It was found that this branch is accompanied by a rapid increase

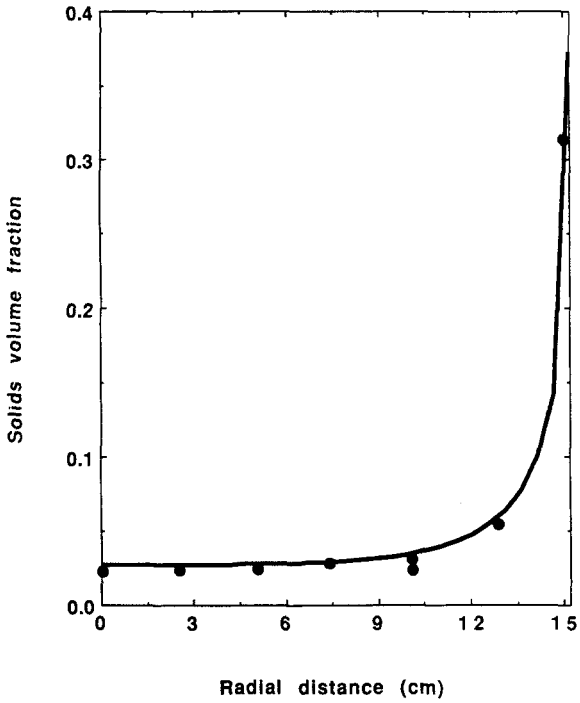

Figure 8. Radial variation of solids volume fraction. $Q_s^* = 98$ kg/m^2·s; $U_g^* = 3.7$ m/s. Tube radius 15.2 cm. The solid circles are the data of Bader et al. (1988).

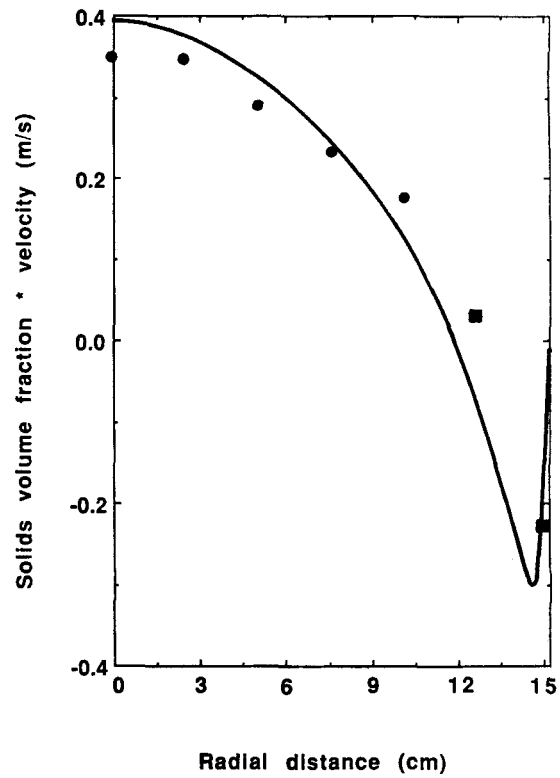

Figure 9. Radial variation of solids mass flux. $Q_s^* = 147$ kg/m^2·s; $U_g^* = 4.6$ m/s; tube radius = 15.2 cm; also shown are the data of Bader et al. (1988).

in the granular temperature and hence the viscosity of the solid phase. Thus, the viscous loss in the solid phase is the more dominant part of the pressure gradient here. It was also found that over the range of gas velocities shown in Figures 7a and 7b, the contribution arising from the effective viscosity of the gas phase is negligible.

Comparison with Experimental Data

Before proceeding with a discussion of the effect of riser diameter, it is worthwhile to compare the model with some experimental data. Figure 8 shows the radial variation of solid volume fraction in a 15.2-cm-radius riser at a Q_s^* of 98 kg/m^2·s and U_g^* of 3.7 m/s. The parameters are as in Table 1 except that $\rho_s = 1{,}714$ kg/m^3 and $d_s = 76$ μm. The figure also shows the data reported by Bader et al. (1988), who carried out experiments in a 10.2-m-tall riser and measured the radial variation of solid fraction at two different heights (4 m and 9 m). The experimental data in Figure 8 are measured at a height of 9 m. The mathematical model with the chosen values for the parameters is able to reproduce the experimental data quite nicely. The sensitivity of the computed results on the chosen values of the parameters was analyzed. It was found that the results are essentially insensitive to small changes in the values of all the parameters except for the coefficient of restitution for particle-particle collisions. This sensitivity will be discussed later.

Figure 9 compares the radial variation of the solid volumetric flux per unit cross-sectional area (i.e., the product of the solid axial velocity and the solid volume fraction) predicted by the

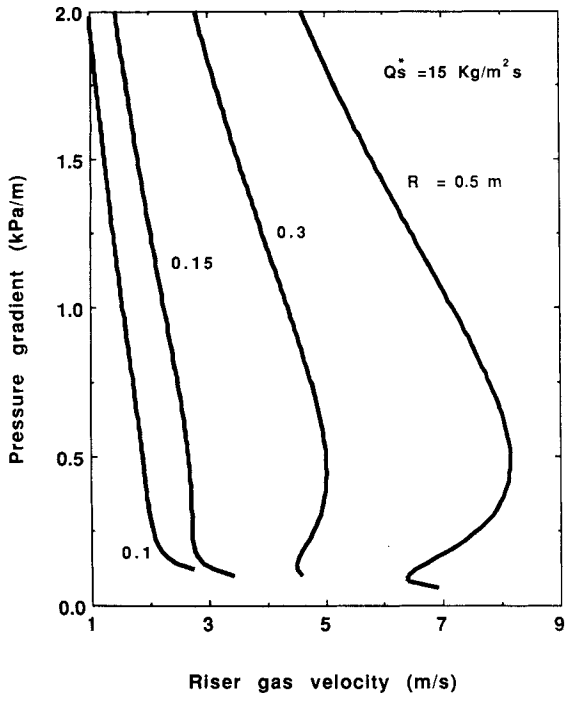

Figure 10. Variation of pressure gradient ($-dp/dz$) as a function of the gas velocity at different tube radii. $Q_s^* = 15$ kg/m^2·s.

model for Q_s^* of 147 kg/m^2·s and $U_g^* = 4.6$ m/s with the experimental data for Bader et al. (1988). The solid circles are the measured values. For regions near the wall, Bader et al. measured the upflow and the downflow and, from these, estimated the net flow that is shown as solid squares. In the core region shown with solid circles, no downflow could be detected experimentally. Again, the mathematical model (with the particular choice of parameters) is able to reproduce the data surprisingly well.

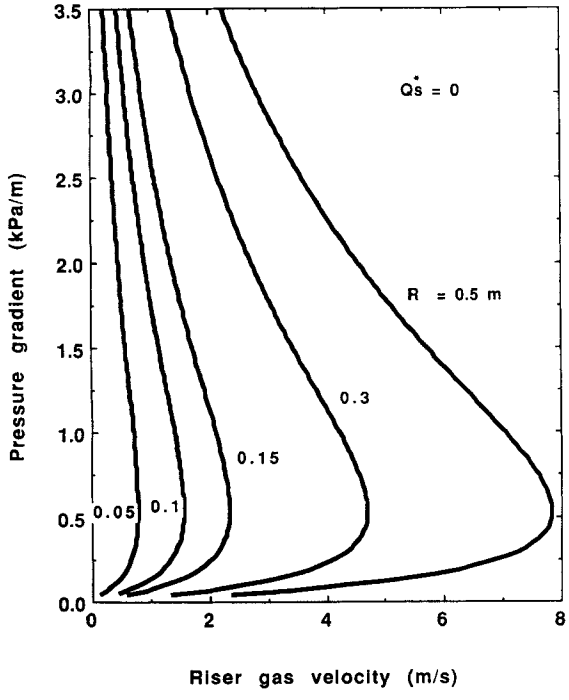

Figure 11. Variation of pressure gradient ($-dp/dz$) as a function of the gas velocity at different tube radii. $Q_s^* = 0$ kg/m^2·s.

Effect of Riser Diameter

Figure 10 shows the variation of $(-dp/dz)$ as a function of U_g^* for different values of riser radius, at $Q_s^* = 15$ kg/m^2·s. Figure 2 shows that for riser radius of 0.5 m, steady-state multiplicity is predicted for a range of riser gas velocities at this solids flux, and this is seen in Figure 10 as well. Note that as the riser radius decreases, the curve shifts dramatically to the left and the multiplicity disappears. This clearly illustrates the potential perils in simple-minded scale-up. The occurrence of steady-state multiplicity is certainly well-known experimentally. It can be concluded from Figure 2 that as one decreases Q_s^*, multiplicity becomes possible for a range of riser gas velocities below a threshold value solid flux, Q_s^{**}. It can be readily inferred from Figure 10 that this threshold value Q_s^{**} must depend on the tube radius. We found that this quantity decreases as the tube radius decreases. As $Q_s^* = 0$ is the lowest value of the solid flux of interest in the context of upflow, it is instructive to construct the plots of $(-dp/dz)$ vs. riser gas velocity for different values of tube radii corresponding to $Q_s^* = 0$, Figure 11. It is seen readily that steady-state multiplicity is present even for small tube diameter. (This figure does not show the lowest branch corresponding to the single-phase gas flow, which is very close to the x-axis.) The range of riser gas velocities for which multiplicity exists increases rapidly as the tube radius increases. Considering that the steady-state multiplicity exists over such a narrow range of flow rates in a 3-cm-dia. tube, it is not surprising that Sinclair and Jackson (1989) failed to notice it.

The variation of $(-dp/dz)$ and average solid holdup as a function of the riser radius is shown in Figure 12a for $Q_s^* = 150$ kg/m^2·s and $U_g^* = 4.5$ m/s. For small tube diameters, an increase in the tube diameter at specified fluxes of gas and solid results in a decrease in the pressure gradient and the solid holdup. This trend is well known (for example, see Yerushalmi

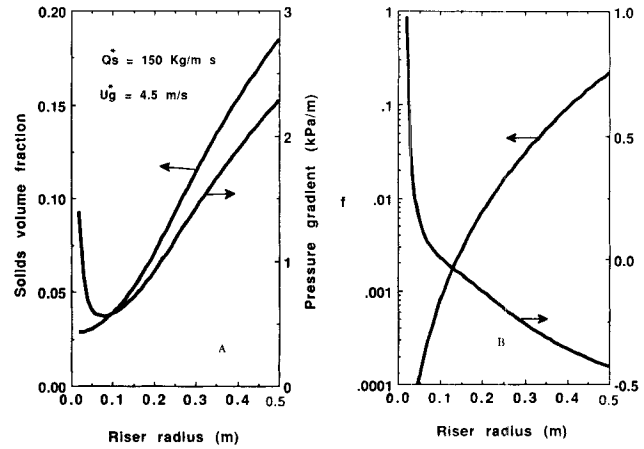

Figure 12. Variation of (a) pressure gradient and the average solids volume fraction, and (b) cross-sectional average of f_1 and the quantity ξ (eq. 16) with the radius of the riser tube. $Q_s^* = 150$ kg/m^2·s; $U_g^* = 4.5$ m/s.

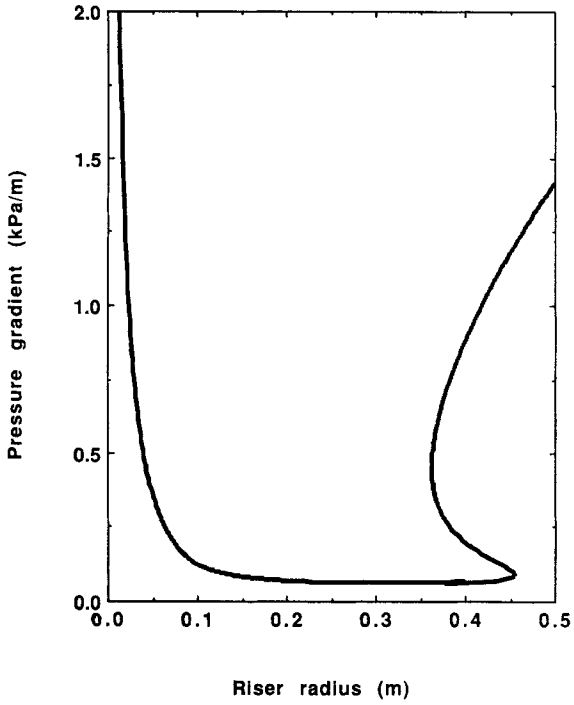

Figure 13. Variation of pressure gradient with the radius of the riser tube for $Q_s^* = 15$ kg/m^2·s and $U_g^* = 6$ m/s.

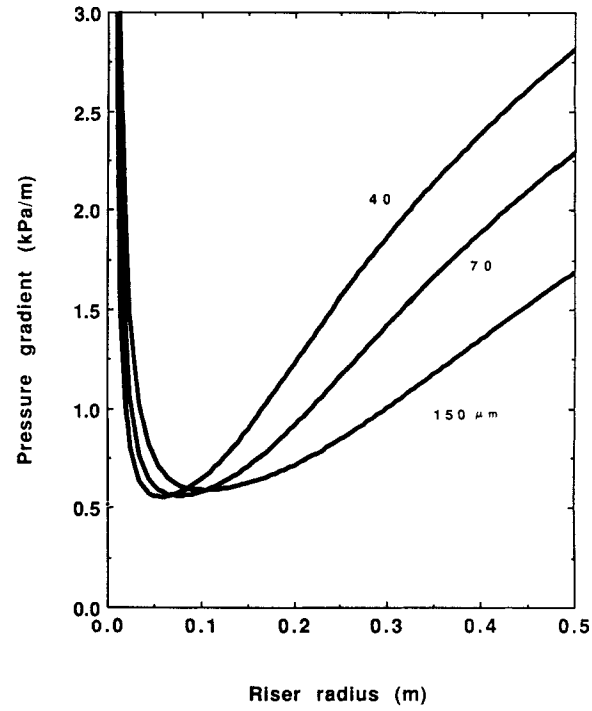

Figure 14. Variation of pressure gradient with the radius of the riser tube for three different values of particle diameters. $Q_s^* = 150$ kg/m^2·s and $U_g^* = 4.5$ m/s.

and Avidan, 1985). The model predicts that somewhere in the range of 5 to 10 cm of tube radius, the trend reverses, as can be seen in Figure 12a. At about the same time, the solid holdup begins to increase rapidly as well. The quantity ξ,

$$\xi = (-dp/dz) - \rho_s g \epsilon_{s,\text{avg}} \tag{16}$$

where $\epsilon_{s,\text{avg}}$ is the average solids volume fraction, is plotted in Figure 12b as a function of the tube radius. For small tubes, this quantity is positive, while for large tubes this quantity becomes negative. For small tube diameters, there is no flow reversal near the tube wall (for this set of fluxes) and hence the wall resistance hinders upflow of the solids. For large tubes, however, there is an appreciable downflow and the wall resistance hinders the downflow of the particles.

Figure 12b also shows the cross-sectional average value of the solid-phase viscosity, $\langle f_1 \rangle$, clearly proving the dramatic increase in the value of this quantity resulting from the rapid increase of the granular temperature with tube diameter. For small tubes, the solid-phase viscosity is small, but the velocity gradient is large. For large tubes, the opposite is true.

Figure 13 shows the variation of $(-dp/dz)$ with the tube radius for a different combination of fluxes ($Q_s^* = 15$ kg/m^2·s and $U_g^* = 6$ m/s). For this combination of fluxes, steady-state multiplicity is observed over a range of tube diameters. The details of flow patterns in the three branches are very similar to those described earlier in Figures 3 to 5.

Effect of Particle Size

The variation of pressure gradient with the riser radius is shown in Figure 14 for three different values of average particle diameter. The pronounced effect of particle size is seen readily. According to the model, in narrow tubes, smaller particles are transported more effectively (i.e., with less pressure gradient); as the tube diameter increases, this trend can reverse! There do not seem to be adequate experimental data to verify if this is indeed true.

Countercurrent Flow and Cocurrent Downflow

It can be seen from Figure 1 that in the countercurrent flow regime, as many as four different values of gas fluxes can be obtained for a given Q_s^* and $(-dp/dz)$ over a range of Q_s^*

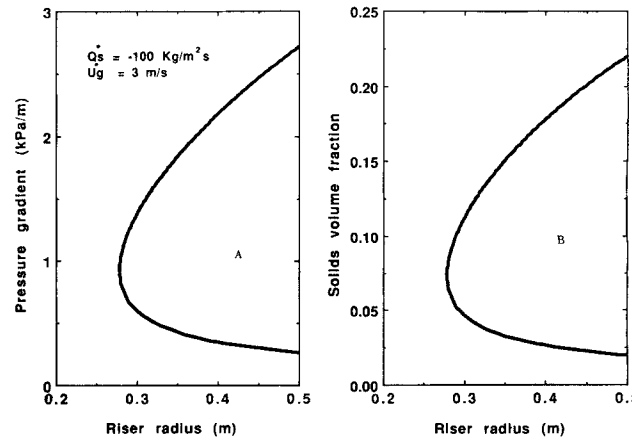

Figure 15. Countercurrent flow. Variation of (a) pressure gradient and (b) average solids volume fraction as a function of tube radius. $Q_s^* = -100$ kg/m^2·s; $U_g^* = 3$ m/s.

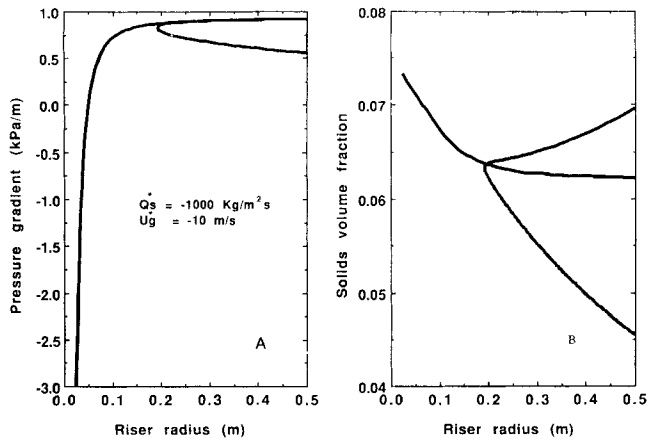

Figure 16. Cocurrent downflow. Variation of (a) pressure gradient and (b) average solids volume fraction as a function of tube radius. $Q_s^* = -1000$ kg/m^2·s; $U_g^* = -10$ m/s.

values. The two solutions in the cross-back region close to the cusp point A representing the classical fluidized bed will disappear even if the tube is inclined slightly (Ocone et al., 1990) and hence may be neglected. Figure 15 shows the variation of pressure gradient $(-dp/dz)$ and average solid holdup as functions of the tube radius for a countercurrent flow. It is interesting to note that fully-developed flow at the indicated combination of fluxes is not possible for tube radii below (about) 0.27 m. If we keep the gas flux fixed and bring the solid flux closer to zero, the curves shown in Figure 15 will shift to the left. Both branches of solutions shown in Figure 15 have similar radial variations, with solids (and gas) going down near the wall and going up in the core region.

Figure 16 shows a similar plot for a cocurrent downflow. For the combination of fluxes shown, there is a unique solution for small-diameter tubes. When $(-dp/dz)$ is less than zero, no recirculation is possible: both the gas and the solid flow downward at all radial positions. As the tube diameter increases, the sign of $(-dp/dz)$ changes and internal recirculation (in the form of gas and solids flowing up in the core and down near the wall) becomes possible. For large tube diameters, another pair of solutions appear as shown in Figure 16. All the three branches have pronounced radial variations in solid volume fraction.

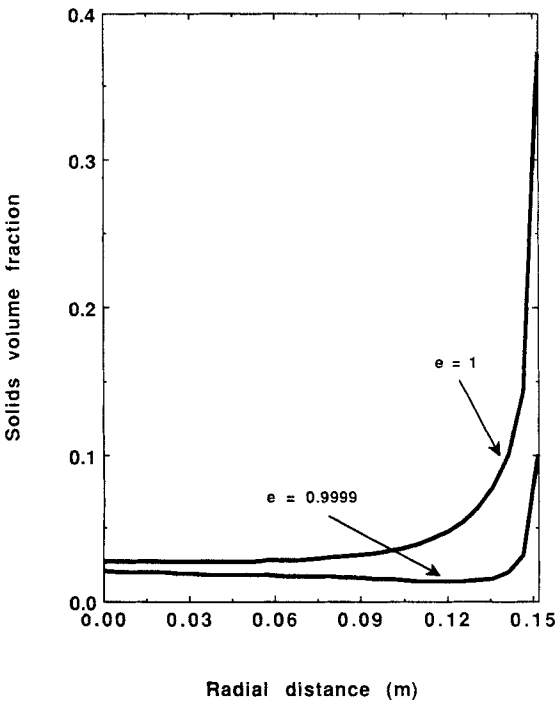

Figure 17. Sensitivity analysis. Radial variation of solid volume fraction for two different values of the coefficient of restitution for the particle-particle collision. Fluxes and tube radius are as in Figure 8.

Discussion

The comparison of the model predictions with the data of Bader et al. (1988) is encouraging. Also, we did not observe any trends in the model predictions that are clearly in violation of what is known empirically. Thus, it is tempting to conclude that the model advanced by Sinclair and Jackson (1989) has captured all the dominant effects. Such enthusiasm, however, is probably not entirely warranted, for reasons discussed below.

It has been assumed in the simulations that the collisions between the particles are elastic. In reality, the particle-particle collisions are far from being elastic. So, one must examine what happens if the value of e is set to be different from unity. This point has been previously addressed by Sinclair and Jackson (1989), who found that the solution structure changed dramatically when e was changed from 1.0 to 0.99. We found the same behavior in our computations for the flow in larger-diameter tubes. To highlight this effect, we have presented in Figure 17 the radial variation of solid fraction for two different values of e, corresponding to the conditions described in Figure 8. Recall that a very good correspondence between the model and the experimental data of Bader et al. (1988) was seen in Figure 8, when we assumed that $e = 1.0$. It can be inferred readily from the enormous sensitivity of the model predictions to the value of e seen in Figure 17 that the agreement displayed in Figure 8 should not be taken too seriously. As repeatedly emphasized by Jackson, the model of Sinclair and Jackson (1989) should not be viewed as being complete.

To understand a second limitation of this model, not reported in the study by Sinclair and Jackson (1989), consider the pseudothermal energy balance, Eq. 4. The second and third terms on the righthand side represent the source of pseudothermal energy arising from the mean shear in particle motion and the sink due to the inelastic particle-particle collisions, respectively. As noted by Buyevich (1971), the fluid-particle interactions do provide a source as well as a sink for pseudothermal energy. Ding and Gidaspow (1990) have proposed the term

$$(-3\beta_{sg}\theta) \tag{17}$$

be added to the righthand side of Eq. 4 to account for the *sink* due to the fluid-particle interaction. They have also argued that the source due to the fluid-particle interaction is not likely to be significant. In Figure 18, we display the radial variation

of the solid volume fraction predicted by the model for two different cases. In both of these cases, we have assumed that e is unity. The gas and solid fluxes are as in Figure 8. Case 1 corresponds to the model as presented by Sinclair and Jackson (1989). When one adds the term suggested by Ding and Gidaspow (1990) (Eq. 17) to the righthand side of Eq. 4, case 2 results. It is clear that the sink term (case 2) can modify the results dramatically. (Note that in the results presented here, fluid-particle interaction is the only sink.)

Louge et al. (1990) have expanded the model of Sinclair and Jackson (1989) to account for the effect of turbulence. They found that if one neglects the source of pseudothermal energy due to the mean shear in the particle motion (i.e., the second term in the right side of Eq. 4) and introduces the contribution arising from turbulence in the fluid phase, the model could not be made to match experiments. Such matching was possible when both the turbulence effect and the source due to the mean shear in the particle assembly were retained. Unfortunately, they did not report what happens if the source due to the mean shear in the particle assembly was retained, but the effect of turbulence was dropped.

Thus, the model of Sinclair and Jackson (1989) analyzed here predicts an unrealistic degree of sensitivity to the coefficient of restitution for particle-particle collisions and the damping of the particle-phase fluctuating motion by the gas phase. This could perhaps be remedied by including the turbulence effects, but this remains to be demonstrated.

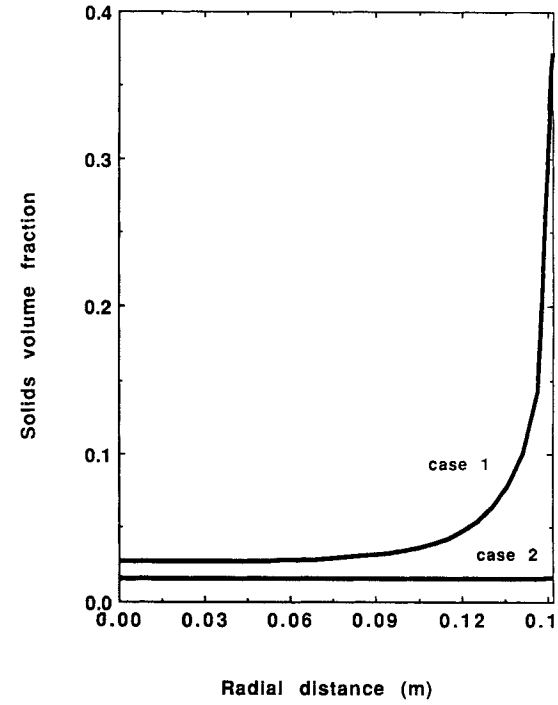

Figure 18. Sensitivity analysis. Radial variation of solid volume fraction with (case 2) and without (case 1) gas phase damping of the particle phase random motion. Fluxes and tube radius are as in Figure 8.

Summary

In the present study, we have expanded the work of Sinclair and Jackson (1989) and investigated the fully-developed flow of gas-particle suspensions in vertical pipes of different diameters. This model predicts a complex scale-up behavior. The new features revealed by our computational analysis are as follows:

- The existence of steady-state multiplicity, in which different pressure gradients can be obtained for the same gas and solid fluxes, has been known experimentally for many years and is indeed predicted by the model of Sinclair and Jackson (1989).
- It is known experimentally that when the tube diameters are small, the pressure gradient required to achieve desired solid and gas fluxes in a riser decreases as the tube diameter increases (Yerushalmi and Avidan, 1985). This was indeed observed in our simulations. When the tube diameters are large, however, this trend can reverse, due to a rapid increase in the fluctuating component of the particle velocity with tube diameter.
- Operations in the countercurrent mode at certain combinations of gas and solid fluxes are possible in large-diameter tubes, but not in small-diameter tubes.
- Scale-up of cocurrent downflow is no less complex than cocurrent upflow. According to the model, while there may be only one steady state for a given combination of fluxes in small-diameter tubes, multiplicity of steady states is possible upon scale-up.

It is also pointed out that the model manifests an unsatisfactory degree of sensitivity to the inelasticity of the particle-particle collisions and the damping of particle-phase fluctuating motion by the gas.

Acknowledgment

We would like to acknowledge many helpful discussions with F. J. Krambeck, A. A. Avidan, A. V. Sapre, D. H. Anderson, and Roy Jackson in preparing this article.

Notation

C_d = drag coefficient described after Eq. 12
d_s = particle diameter, m
e = coefficient of restitution for particle-particle collisions
e_w = coefficient of restitution for particle-wall collisions
f_1 = effective viscosity of the particle phase, Eqs. 5 and 10, kg/m·s
f_2 = effective pseudothermal conductivity, Eqs. 7 and 11, kg/m·s
g = acceleration due to gravity, m/s^2
g_o = radial distribution function
m = mass of a single particle, kg
p = gas pressure, kPa
q_{PT} = pseudothermal energy flux, kg/s^3
Q_s^* = mass flux of particles (cross sectional average), kg/m^2·s
r = radial coordinate, m
R_t = tube radius, m
Re_g = gas phase Reynolds number based on particle diameter
S = particle phase stress tensor, kg/m·s^2
U_g, U_s = local average axial velocities of gas and particles, m/s
U_g^* = superficial velocity of the gas, m/s
U_t = terminal velocity of the particle, m/s

Greek letters

β_{sg} = drag coefficient defined by Eq. 12, kg/m^3·s
γ = dissipation rate of pseudothermal energy due to inelastic collisions between particles, Eq. 8, kg/m·s^3
δ, δ_o = see Eq. 15

ϵ_g, ϵ_s = local average volume fractions of gas and solid, $\epsilon_g + \epsilon_s = 1$
ϵ_o = maximum possible value for ϵ_s
η = see Eq. 12
θ = granular (particle) temperature, m^2/s^2; except in Eq. 3 where it defines one of the azimuthal direction
λ = see Eq. 12, kg/m·s
μ, μ_b = see Eq. 12, kg/m·s
μ_g = viscosity of the gas, kg/m·s
μ_{eg} = effective viscosity of the gas phase, Eq. 9, kg/m·s
ξ = see Eq. 16
ρ_g, ρ_s = density of gas and solid, kg/m^3
σ_{ij} = components of the stress tensor associated with the particle assembly, defined in the compressive sense
ϕ' = specularity coefficient for particle-wall collisions

Literature Cited

Arastoopour, H., and C. Cutchen, "Measurement and Analysis of Particle-Particle Interaction in Cocurrent Flow of Particles in a Dilute Gas-Solids System," *Chem. Eng. Sci.*, **40**, 1135 (1985).

Arastoopour, H., C. Wang, and S. Weil, "Particle-Particle Interaction Force in a Dilute Gas-Solids System," *Chem. Eng. Sci.*, **37**, 1379 (1982).

Bader, R., J. Findlay, and T. M. Knowlton, "Gas/Solid Flow Patterns on a 30.5-cm-Diameter Circulating Fluidized Bed," Int. Circulating Fluidized-Bed Conf., Compiegne, France (Mar. 14-18, 1988).

Batholomew, R., and R. Casagrande, "Measuring Solids Concentration in Fluidized Systems by Gamma Ray Absorption," *Ind. Eng. Chem.*, **49**, 428 (1957).

Berker, A., and T. Tulig, "Hydrodynamics of Gas-Solids Flow in a Catalytic Cracker Riser: Implications for Reactor Sensitivity Performance," *Chem. Eng. Sc.*, **41**, 821 (1986).

Buyevich, Y. A., "Statistical Hydrodynamics of Disperse Systems: 1. Physical Background and General Equations," *J. Fluid Mech.*, **49**, 489 (1971).

Chen, Y-M., S. Rangachari, and R. Jackson," A Theoretical and Experimental Investigation of Flow in a Vertical Standpipe," *Ind. Eng. Chem. Fundam.*, **23**, 354 (1984).

Contractor, R. M., and A. W. Sleight, "Selective Oxidation in Riser Reactor," *Catalysis Today*, **3**, 175 (1988).

Ding, J., and D. Gidaspow, "A Bubbling Fluidization Model Using Kinetic Theory of Granular Flow," *AIChE J.*, **36**, 523 (1990).

Gidaspow, D., and C. Solbrig, "Transient Two-Phase Flow Models in Energy Production," AIChE Meeting (1976).

Ginestra, J. C., S. Rangachari, and R. Jackson, "A One-Dimensional Theory of Flow in Vertical Standpipes," *Powder Technol.*, **27**, 69 (1980).

Hinze, J., "Momentum and Mechanical Energy Balance Equations for a Flowing Homogeneous Suspension with Slip Between the Two Phases," *Appl. Sci. Res.*, **11**, 33 (1962).

Leung, L. S., and P. Jones, "Coexistence of Fluidized Solids Flow and Packed Flow in Standpipes," *Proc. Int. Fluidization Conf.*, **116**, Cambridge Univ. Press (1978).

Louge, M., E. Mastorakos, and J. T., Jenkins, "The Role of Particle Collisions in Pneumatic Transport," No. 165j, AIChE Meeting, Chicago (Nov., 1990).

Lun, C., S. B. Savage, D. Jeffrey, and N. Chepurny, "Kinetic Theories for Granular Flow: Inelastic Particles in Couette Flow and Slightly Inelastic Particles in a General Flow Field," *J. Fluid Mech.*, **140**, 223 (1984).

Ocone, R., S. Sundaresan, and R. Jackson, IFPRI Annual Report ARR 09-08 (Nov., 1990).

Saxton, A., and A. Worley, "Modern Catalytic Cracking Design," *Oil and Gas J.*, **68**, 82 (1970).

Sinclair, J. L., and R. Jackson, "Gas-Particle Flow in a Vertical Pipe with Particle-Particle Interactions," *AIChE J.*, **35**, 1473 (1989).

Weinstein, H., M. Shao, and L. Wasserzug, "Radial Solid Density Variation in a Fast Fluidized Bed," *AIChE Symp Ser.*, **80**, 117 (1984).

Yerushalmi, J., M. Cankurt, D. Geldart, and B. Liss, "Flow Regimes in Vertical Gas-Solid Contact Systems," *AIChE Symp. Ser.*, **74**, 1 (1978).

Yerushalmi, J., and A. A. Avidan, "High Velocity Fluidization," in *Fluidization*, 2nd ed., J. F. Davidson, R. Clift, and D. Harrison, eds., Academic Press, p. 225 (1985).

Youchou, L., and M. Kwauk, "The Dynamics of Fast Fluidization," *Fluidization*, J. Grace and J. Matsen, eds., Plenum Press, New York (1980).

Wirth, K-E., "Axial Pressure Profile in Circulating Fluidized Beds," *Chem. Eng. Technol.*, **11**, 11 (1988).

Manuscript received Apr. 22, 1991.